Experiment S-10: Optical Pumping

Physics 510

Darren Puigh
(Dated: February 27, 2006)

This experiment used the process of optical pumping to investigate the hyperfine splitting of two rubidium isotopes in the presence of an external magnetic field. The magnetic field caused a splitting in the energy of the m_F magnetic sublevels. Shining a source of optical photons through a chamber containing ^{85}Rb and ^{87}Rb vapor resulted in the atoms being pumped into the state of highest m_F. The level to which the sample had been pumped was determined by measuring the intensity of optical photons that passed through the vapor. When photons of the right energy (corresponding to radio frequencies) interacted with the atoms, they would transition out of the state of highest m_F. The absorption of the pumping photons would then increase, and the photodiode current would decrease. Utilizing this technique, the Landé g_F factors for ^{85}Rb and ^{87}Rb were found to be 0.335 ± 0.008 and 0.505 ± 0.006, respectively, in good agreement with theoretical values of 0.334 and 0.500. Simultaneously, the magnetic field of the Earth was measured to be 0.496 ± 0.029 Gauss. Investigations into the characteristic time required to establish steady state polarization of the spins yielded that this time was independent of the light intensity. The characteristic times for r.f. fields of frequency 1.005 MHz, 0.900 MHz, and 0.800 MHz were determined to be 11.5 ± 0.4 ms, 12.6 ± 0.6 ms, and 12.8 ± 0.6 ms, respectively. In addition, it was also observed that there was an apparent resonance when the total field seen by the sample was swept through zero. By varying the amplitude of the r.f. field, the difference between sudden and adiabatic passage through resonance was studied quantitatively.

INTRODUCTION

The process of optical pumping has been around for more than half a century. Its name refers to the preparation of the sample. It indicates that an equilibrium population of states will be "pumped" upon until only the higher energy states are occupied. This process is accomplished through the absorption/emission of optical photons. Once this nonequilibrium population is established, it can be used in a variety of ways. Optical pumping has led to many important developments, such as lasers, sensitive magnetometers, and atomic clocks. For this experiment, it was used to examine the hyperfine structure of atomic states.

It is well known that there are many corrections to the Bohr atom. There is a fine structure to the hydrogen atom energies due to two different mechanisms: electron spin-orbit coupling and a relativistic correction. Due to this coupling of the spin, $\vec{S}$, and orbital angular momentum, $\vec{L}$, we find it necessary to use eigenstates of total angular momentum $\vec{J}$, where $\vec{J} = \vec{L} + \vec{S}$ [1]. Once these corrections have been taken into account, we see that the fine structure breaks the degeneracy in l; the energies are now determined by the quantum numbers n and j.

In addition to the fine structure, there is also a correction due to the spin of the nucleus and its magnetic dipole moment. Just as before, this interaction causes neither the nuclear spin, $\vec{I}$, nor the electron's total angular momentum, $\vec{J}$ to be constants of motion (they are not eigenstates of the perturbation). Only the total angular momentum of the atom, $\vec{F}$, is conserved, where $\vec{F} = \vec{I} + \vec{J}$. There is now a splitting in the energy levels of different F. This is the hyperfine splitting. The application of a weak external magnetic field results in the Zeeman spliting of these F states, lifting the degeneracy in the m_F magnetic sublevels. Now, the only orientations of F allowed are the ones that have projections along the direction of the magnetic field, m_F, that take on an integer value between F and - F. In principle, higher order multipole terms other than the magnetic dipole would also contribute to the hyperfine structure. However, since the nuclear dimensions are so much smaller than atomic dimensions, the contribution to the energy drops rapidly with multipole order [2]. Figure 1 displays the level diagram for ^{87}Rb when considering only the dipole hyperfine structure. One goal of our experiment was to determine the relation between the energy splittings in the m_F magnetic sublevels and the applied magnetic field using rubidium.

In order to measure the transition between one sublevel and another, we first had to prepare the atoms such that only one sublevel was occupied. This is complicated by the fact that the relevant energy differences between adjacent sublevels correspond to photons in the radio frequency band of the electromagnetic spectrum. The separation is so small that thermal excitations and collisions will cause each level to be nearly equally populated. This is where optical pumping becomes important. Optical pumping is based on energy and momentum conservation, as well as the selection rules for magnetic dipole transitions. Consider the case of ^{87}Rb (I = 3/2). Imagine that the sample atoms are all in the $^2S_{1/2}$ state with F = 0 or 1. Initially, all sublevels are nearly equally occupied in the presence of a weak magnetic field. The

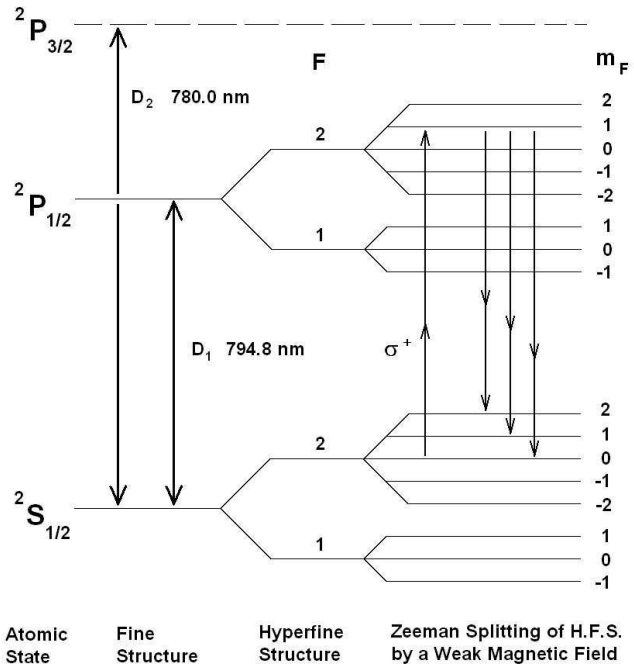

FIG. 1: Level Diagram for ^{87}Rb (I = 3/2) as different corrections are considered. For simplicity, the hyperfine structure and Zeeman splitting of the $^2P_{3/2}$ state are not shown. Included in the diagram are the possible transitions of an atom initially in the F = 2, $m_F = 0$ sublevel of the ground state after absorption of a photon with one unit of angular momentum and spontaneously emitting a photon of random polarization.

objective is to get all atoms into the F = 2, $m_F = 2$ state of the groundstate.

One can accomplish this by first shining circularly polarized light through the vapor corresponding to a transition between the $^2S_{1/2}$ state and the $^2P_{1/2}$ state (D_1 radiation). The selection rules involving the absorption or emission of magnetic dipole radiation are $\Delta F = 0$ or ± 1 and $\Delta m_F = 0$, or ± 1 [3]. If the light is right circularly polarized and traveling parallel to the magnetic field, it is denoted σ^+. From momentum conservation, absorption of σ^+ light by an atom raises m_F by 1 unit. Once the atom is in the excited state, it will spontaneously emit radiation of random polarization resulting in an equal probability of m_F increasing by 1, decreasing by 1, or staying the same. The net result of the absorption and then emission of one D_1 photon is $\Delta m_F > 0$ with 2/3 probability or $\Delta m_F = 0$ with 1/3 probability. Figure 1 illustrates one such cycle.

This process is repeated with each incident photon. If relaxation processes are slow compared to the rate of "pumping", the atoms will all be pumped into the F = 2, $m_F = 2$ state of the groundstate, as desired. The atoms in this state can no longer absorb the D_1 radiation, because there is no $m_F = 3$ sublevel in the $^2P_{1/2}$ state. However, such a state does exist when transitioning from the ground state to $^2P_{3/2}$ is allowed (through absorption of D_2 radiation). Therefore, D_2 light must be filtered to prevent this escape route from the $m_F = 2$ state.

The previous discussion was based on ^{87}Rb, but natural rubidium contains both ^{85}Rb and ^{87}Rb, with nuclear spins 5/2 and 3/2, in the ratio 72 to 28%, respectively. Thus, with one chamber of rubidium vapor, it was possible to investigate the field dependence of the Zeeman splittings of both isotopes simultaneously.

THEORETICAL BACKGROUND

Zeeman Splitting of Hyperfine Structure

When we determine the relation between Zeeman energy splittings and weak magnetic fields, specifically we are measuring the Landé g-factor, also known as the gyromagnetic ratio. The g-factor relates the magnetic dipole moment to the angular momentum of a quantum state. With angular momentum in units of $\hbar$, we have the following equations relating magnetic dipole moment to angular momentum [4]:

$$\vec{\mu}_S = -g_S\,\mu_B\,\vec{S}, \tag{1}$$
$$\vec{\mu}_L = -g_L\,\mu_B\,\vec{L}, \tag{2}$$
$$\vec{\mu}_J = -g_J\,\mu_B\,\vec{J}, \tag{3}$$
$$\vec{\mu}_I = \;\; g_I\,\mu_N\,\vec{I}, \tag{4}$$
$$\vec{\mu}_F = -g_F\,\mu_B\,\vec{F}, \tag{5}$$

where μ_B and μ_N are the Bohr and nuclear magneton, respectively. Given the relations (1) - (3) and $\vec{J} = \vec{L} + \vec{S}$, and using the properties of the dot product, one obtains

$$g_J\,J = g_L\,L\,cos\,\theta_{JL} + g_S\,S\,cos\,\theta_{JS} \tag{6}$$

with θ_{AB} representing the angle between the vectors $\vec{A}$ and $\vec{B}$. Similarly, one can use the equation for the total angular momentum of the electron J to get

$$\vec{L}^{\,2} = \vec{S}^{\,2} + \vec{J}^{\,2} - 2SJ\,cos\,\theta_{JS}, \tag{7}$$
$$\vec{S}^{\,2} = \vec{L}^{\,2} + \vec{J}^{\,2} - 2LJ\,cos\,\theta_{JL}. \tag{8}$$

Quantum mechanically, the expectation value for the angular momentum of $\vec{A}^{\,2}$ is A(A+1). In the end, solving (7) and (8) for the cosine of the angles and substituting the result into (6) yields

$$g_J = g_S\frac{J(J+1)+S(S+1)-L(L+1)}{2J(J+1)} + g_L\frac{J(J+1)+L(L+1)-S(S+1)}{2J(J+1)} \tag{9}$$

For this experiment, we are studying the Zeeman splitting of the groundstate. Here L = 0 and J = S = 1/2.

Therefore, $g_J = g_S$. Similarly, one can use the exact same procedure for the total angular momentum of the atom to find that it has a g-factor

$$g_F = g_J \frac{F(F+1) + J(J+1) - I(I+1)}{2F(F+1)} - g_I \frac{F(F+1) + I(I+1) - J(J+1)}{2F(F+1)} \quad (10)$$

We are interested in the case where F = 2 and J = 1/2. Substituting these values and $g_J = g_S$ into (10) for ^{85}Rb (I = 5/2), we find

$$g_F = -\frac{1}{6}\left(g_S + 7g_I\right), \quad (11)$$

and for ^{87}Rb (I = 3/2) we find

$$g_F = \frac{1}{4}\left(g_S - 3g_I\right). \quad (12)$$

The negative sign on (11) indicates that decreasing values of m_F yield higher energy levels. Using the method of optical pumping, we will be determining the absolute value of g_F. Thus, we will only be quoting positive values of g_F.

Experimentally, the gyromagnetic ratio of the electron has been measured, yielding a value $g_S = 2.002319304$ [5]. In addition, the nuclear to electronic g-factor ratio, g_I/g_J, for ^{85}Rb has been determined to be $1.46649093(11) \times 10^{-4}$, independent of magnetic field [6]. Assuming that ^{87}Rb has a similarly small g-factor ratio, then (11) and (12) provide theoretical predictions (to 3 significant figures) of $g_F = 0.334$ and $g_F = 0.500$ for ^{85}Rb and ^{87}Rb, respectively. The number of significant figures was chosen to correspond with the precision to which this experiment was performed and to emphasize the fact that calculations are valid only to first order.

Finally, the Zeeman energy splitting of m_F sublevels in a weak magnetic field is (to first order) given by [1]

$$E = g_F \frac{e\hbar}{2m_e} B\, m_F = g_F\, \mu_B\, B\, m_F. \quad (13)$$

Establishing Steady State Polarization

After the rubidium atoms have been subjected to a radio frequency (r.f.) field of the right energy to induce a transition, the intensity of the D_1 radiation passing through the rubidium vapor will drop sharply. Once this r.f. field is removed, the atoms will be pumped on again until a steady state polarization is established. There is a characteristic time associated with this phase. Following Benumof [4], we can determine the change in population of the $m_F = 3$ groundstate of ^{87}Rb relative to the other sublevels. This can be written as

$$\frac{dn}{dt} = -nW_d + NW_u \quad (14)$$

where n is the population of the $m_F = 3$ sublevel and N is the population of every other sublevel. The rate of transitioning down out of the pumped state is given by W_d, and W_u is the rate of transitioning into $m_F = 3$. The characteristic time to establish steady state polarization is found from (14).

Do we expect this time to depend on the intensity of the light? Clearly, the relaxation processes causing the transition out of the pumped state, W_d, should not depend on the light intensity. W_d is a result of the atoms colliding with the glass walls. Next, we can break up W_u into two different steps. This rate depends both on the rate of transition into the $^2P_{1/2}$ excited state, $\Gamma_\uparrow$, and the rate of transition back down into the $m_F = 3$ groundstate, $\Gamma_\downarrow$. The longer rate, $\Gamma_\uparrow$ or $\Gamma_\downarrow$, will determine W_u. The intensity of the light is a measure of rate that optical photons are incident on the sample. Since these photons are responsible for excitation of the groundstate, $\Gamma_\uparrow$ will depend directly on the intensity. However, the transition back to the groundstate is caused by the spontaneous emission of the optical photon. From the Fermi's Golden Rule [2], the spontaneous emission should depend on the frequency of the emitted photon and not the intensity of the light. We expect timescales of spontaneous emission to be much longer than those of photon absorption from the light. Therefore, the characteristic time should not depend on intensity.

Dynamic Response of Spins to Time Varying Magnetic Fields

We wish to first discuss passage through zero field (applied field canceling the Earth's Field) in the absence of any r.f. field. In a static coordinate system, the nuclear spins obey the classical equation of motion [7]

$$\frac{d\vec{I}}{dt} = \gamma\left(\vec{I} \times \vec{B}\right). \quad (15)$$

Due to the variation of $\vec{B}$ with time, this is a difficult problem to solve. For instructive purposes, we examine limiting cases. The magnetic field vector can be separated into components perpendicular and parallel to the axis of the primary Helmholtz coils. The two cases [8] are adiabatic passage throug zero field given by

$$\frac{1}{B_\perp}\frac{dB_\parallel}{dt} \ll \gamma B_\perp, \quad (16)$$

and sudden passage given by

$$\frac{1}{B_\perp}\frac{dB_\parallel}{dt} \gg \gamma B_\perp. \quad (17)$$

If the magnetic field is varying slowly, then (16) is satisfied, and $\vec{I}$ will stay nearly parallel with $\vec{B}$. As $\vec{B}$ is swept through zero, so is $\vec{I}$, and the z-component of $\vec{I}$

will reverse sign. This will be as if the pumping light was reversed [4]. Light that was right-circularly polarized and resulted in raising m_F by one unit will now remove one unit of angular momentum. The pumping process will begin again, pumping atoms in the opposite way as before, and absorption of D_1 light will increase dramatically. When this happens, there will be a large optical signal.

On the other hand, it might be the case that the sweep rate of the magnetic field is too fast for the magnetization to follow. In this situation, (17) is satisfied. Now, magnetization remains always pointed in the same direction. So, when the field changes sign, it did so quickly enough to not affect the spins. Therefore, right-circularly polarized light will still increase m_F by one unit. The net result is that pumping remains unchanged, so the optical signal is relatively steady.

When considering a resonance in the presence of a r.f. magnetic field, it is useful to tranform into a rotating coordinate system. Here, we wish to transform into a coordinate frame that rotates at the frequency of the r.f. field. The rate of change for any vector in a fixed reference frame is given by [9]

$$\left(\frac{d\vec{I}}{dt}\right)_{fixed} = \vec{\omega} \times \vec{I} + \left(\frac{d\vec{I}}{dt}\right)_{rotating}. \qquad (18)$$

Using this translation along with (15), it can be shown [8] that $B_\perp$ becomes replaced by $B_{r.f.}$. If we define the quantity

$$X \equiv \frac{\mu_B}{\gamma} \frac{1}{B_{r.f.}^2} \frac{dB_\parallel}{dt}, \qquad (19)$$

then the adiabatic and sudden conditions can be written as $X \ll 1$ and $X \gg 1$, respectively. Although the argument above was based on classical mechanics, the result holds quantum mechanically [7].

EXPERIMENTAL SETUP

The layout for this experiment is shown in Figure 2. Two sets of Helmholtz coils were used to provide the weak external magnetic field. The primary coils (shown in the figure) were aligned so that they would produce a magnetic field either parallel or anti-parallel to the Earth's magnetic field. Secondary coils were placed at right angles to these fields in an effort to minimize the transverse field and its inhomogeneities. Current through the primary coils was controlled with a trapezoidal sweep by using a function generator and control circuit.

Production of circularly polarized waves was achieved by using a linear polarizer and a quarter-wave plate. The two were aligned to obtain maximal circular polarization

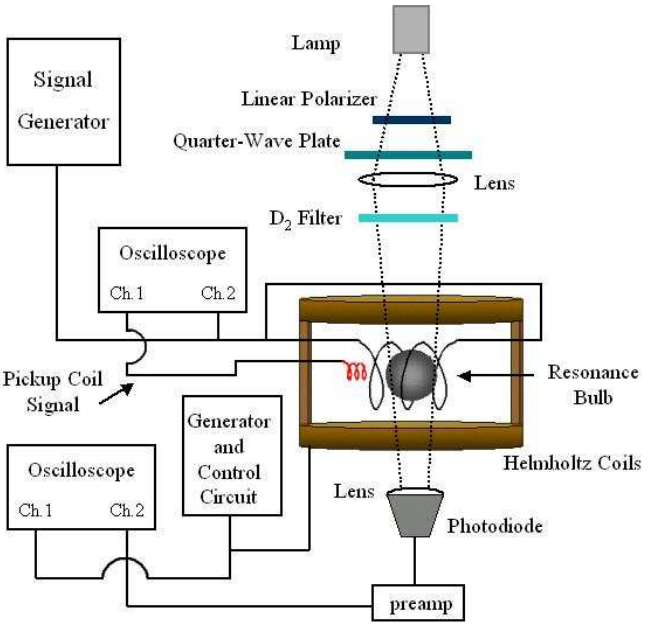

FIG. 2: Diagram of optical pumping setup. Only the primary Helmholtz coils are shown in this diagram. The secondary coils used to trim the transverse fields to zero are not shown.

of optical light from a lamp. The D_2 radiation was removed from the light for the previously mentioned reasons. A converging lens focused the light going through a resonance bulb full of rubidium vapor. Due to the low melting point of rubidium (38.5 °C), the resonance bulb was heated by blowing hot air onto it to achieve optimum vapor pressures.

A signal generator supplied the radio frequency field necessary to induce transitions out of the pumped state. The magnitude of the r.f. field was determined by measuring the emf induced in a small pickup coil. For each frequency, the magnetic field from the primary Helmholtz coils was swept through a range of values. When the magnetic field passed through resonance for a given isotope satisfying (13), absorption of the D_1 radiation increased sharply. Since the sweep of the primary coils was trapezoidal, there were two peaks for each isotope during one period of the sweep. Figure 3 shows both the sweep and the resonant peaks for each isotope at a fixed frequency. For all measurements, the oscilloscope was run in `Average 256` mode to reduce the amount of noise in the signal.

In order to determine the effect of light intensity on the characteristic time to establish steady state polarization, it was necessary to vary the amount of incident light. This was achieved by placing a second linear polarizer between the lamp and the first linear polarizer. By varying the the angle between the two polarizers, it was possible to control the intensity of light shining on the sample.

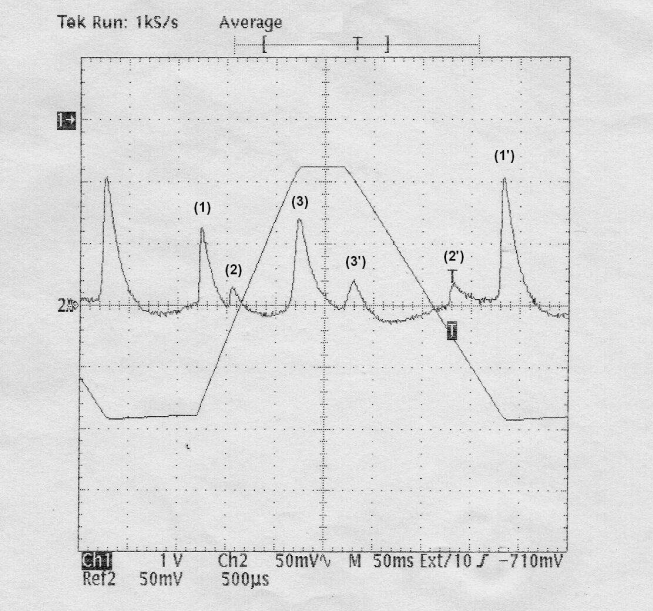

FIG. 3: Oscilloscope trace of resonant peaks at a frequency of 1.005 MHz. Ch. 1 - Trapezoidal sweep for the primary Helmholtz coils. Ch. 2 - Signal from the photodiode. Peaks (1) and (1') correspond to ^{85}Rb, and peaks (2) and (2') correspond to ^{87}Rb. Note the appearance of an extra pair of peaks (3) and (3') corresponding to zero applied field.

RESULTS AND DISCUSSION

The magnetic field due to the primary Helmholtz coils was determined from the geometry of the coils and the amount of current flowing through them. These coils were designed to provide as uniform of a field as possible. To that end, the separation between the coils was measured to be the same (up to uncertainty) as the radius of each coil. Therefore, the magnetic field (in Tesla) in between and on the axis the coils is given by [10]

$$B = \left(\frac{4}{5}\right)^{3/2} \frac{\mu_0 N I}{r}, \tag{20}$$

where N is the number of turns in the coil and r is the radius of the coils. The energy level splitting was determined by measuring the frequency of the r.f. field and using $E = h\nu$.

The relationship between the Zeeman energy splitting and applied magnetic field for both isotopes of rubidium is shown in Figure 4. The two lines were found using a least-squares weighted fit [11]. The magnetic field B was graphed vs. the energy E, instead of the reverse, due to the larger error in measurements of B. The slope of each line determined the value of $(g_F\,\mu_B)^{-1}$, from which the g-factor could be obtained. In addition, the y-intercept of each line is a measure of the Earth's magnetic field. According to (13), one would expect the zero of energy

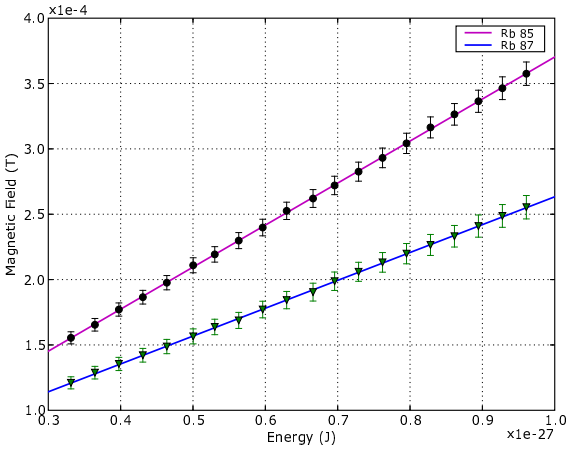

FIG. 4: Finding the g_F values for ^{85}Rb and ^{87}Rb. The slope of these lines represent the $(g_F\,\mu_B)^{-1}$. The y-intercept of each line (not shown) was used to infer the magnitude of the Earth's magnetic field. Resonance measurements for twenty different frequencies were used.

TABLE I: G-factor measurements for two rubidium isotopes. Also included is the magnitude of the Earth's magnetic field determined using each isotope.

Rb Isotope	g_F	$B_{Earth}(G)^a$
85	0.335 ± 0.008	0.488 ± 0.046
87	0.505 ± 0.006	0.501 ± 0.050

[a]Weighted average yields 0.496 ± 0.029 G.

splitting to occur in the presence of zero applied magnetic field. The fact that the y-intercept is not zero indicates that there is an additional magnetic field other than the one produced by the Helmholtz coils. This extra field is attributed solely to field of the Earth. From the y-intercepts of both lines, we obtain a weighted average for the Earth's magnetic field of 0.496 ± 0.029 G. Table I summarizes the results.

The characteristic time, τ, to establish steady state polarization was measured for different frequencies and intensities. Assuming an exponential decay of photodiode signal, the logarithm of the voltage was graphed versus time so that the points would fit a straight line with slope τ^{-1}. Again, each line was created using a least-squares weighted fit. Figure 5 displays the results at a fixed frequency of 0.900 MHz. Notice that each line has approximately the same slope. Table II provides the characteristic time for different polarizations. These characteristic times are all in good agreement, indicating that τ does not depend upon the light intensity, as hypothesized.

The measured values of τ and their uncertainties for each intensity and for three different frequencies are detailed in Table III. Note that each of the variations of τ

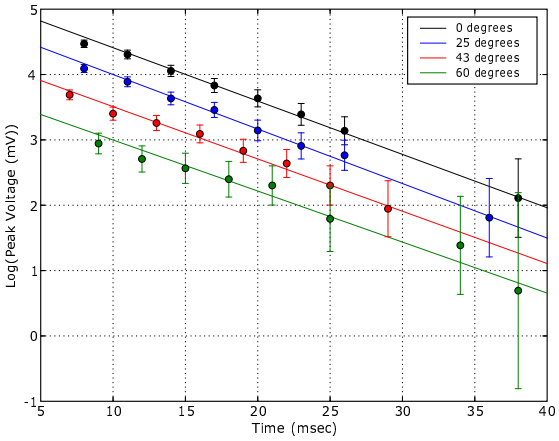

FIG. 5: Dependence of τ on light intensity at 0.900 MHz. The different lines indicate different intensities. It was assumed that the decay of the voltage reading from the photodiode was exponential. Therefore, the slope of each line is τ^{-1}. The fact that these lines are roughly parallel suggests that τ is insensitive to changes in intensity.

TABLE II: Characteristic time to establish steady state polarization at 0.900 MHz.

$\Delta\,\theta$ (deg)[a]	$\frac{I}{I_0}$[b]	τ(ms)
0.	1.00	12.6 ± 1.0
25	0.82	12.3 ± 1.1
43	0.53	12.9 ± 1.4
60	0.25	13.4 ± 2.8

[a]Approximate. Each value has an estimated uncertainty of 3°
[b]Intensity related to angle between polarizers by I = I_0 $\cos^2(\Delta\theta)$.

over the range of intensities agree with zero, suggesting that there is no dependence of τ on light intensity.

In addition to the peaks corresponding to the two rubidium isotopes, it was observed that there was another apparent resonance when the field was swept through zero (applied field canceling the earth's field) in the absence of an r.f. field. See the *Theory* section for explanation.

Figure 6 shows the dependence of the peak voltage on

TABLE III: Characteristic time and its variation per degree separation between linear polarizers for three frequencies.

frequency (MHz)	τ (ms)[a]	$\frac{\Delta\tau}{\Delta\theta}$(ms/deg)
1.005	11.5 ± 0.4	-0.002 ± 0.026
0.900	12.6 ± 0.6	0.016 ± 0.034
0.800	12.8 ± 0.6	0.018 ± 0.033

[a]Weighted average from each polarization.

TABLE IV: Measurements of the peak voltage for different r.f. field strengths. Included is the defined variable X which provides a measure of sudden passage ($X \gg 1$) and adiabatic passage ($X \ll 1$).

Peak (mV)[a]	$B_{r.f.} \times 10^{-7}(T)$	X[b]
14	0.14	216.
27	0.28	54.0
44	0.39	27.5
61	0.50	16.7
78	0.72	7.98
93	0.99	4.16
95	1.21	2.79
103	1.49	1.85
103	1.71	1.40
107	1.98	1.04
109	2.48	0.67
110	3.03	0.45
110	3.47	0.34
110	3.86	0.28
112	4.41	0.21
113	4.96	0.17

[a]Uncertainty on each peak measurement estimated to be 4 mV.
[b]See equation (19) for definition. $\frac{dB}{dt}$ = 0.001207 T/s.

the magnitude of the r.f. field. For large values of the r.f. field, the adiabatic condition ($X \ll 1$) is satisfied and the peak voltages reach a constant value as the the nuclei preserve their orientation relative to the magnetic field. As the r.f. field gets smaller, the sudden condition ($X \gg 1$) is satisfied and the peak voltage goes to zero as the magnetization has no opportunity to follow the fields. Table IV lists the measured peak voltage for 16 different values of the r.f. field. The value of X (19) is listed for each peak entry.

Error Analysis

There were many sources of error in this experiment. The above figures were displayed such that the quantity with the largest uncertainty was used as the y-axis. In the measurement of g_F for each isotope, the biggest source of error was in the magnetic field corresponding to resonance. Due to the nonuniformities of the magnetic field, it was difficult to ascertain where exactly resonance occurred. It was necessary to average the location of the peaks on both sides of the trapezoidal sweep to achieve the most accurate value of the magnetic field.

Once a value was decided upon, it still had two sources of uncertainty: voltage measurements on the oscilloscope and the radius of the coils. Voltage readings from the oscilloscope had to be translated into current in the primary coils. Then, the current was used to determine the

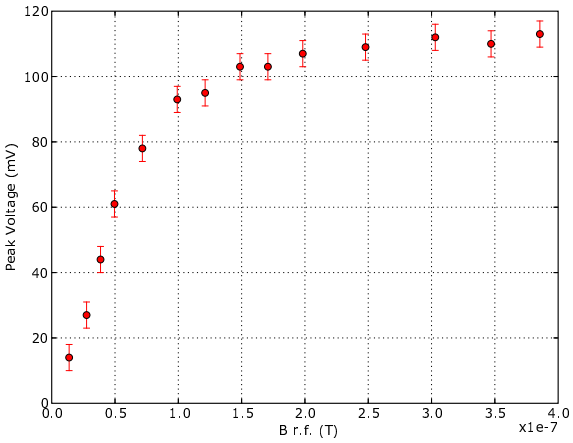

FIG. 6: Sudden vs. adiabatic passage through resonance. Above a certain r.f. field strength, the peak voltages were roughly equal (adiabatic passage). However, decreasing the r.f. field eventually led to attenuation of the peak voltages (sudden passage).

magnetic field. Using standard procedures of error propagation [11], it was possible to determine a reasonable measure of uncertainty in each measurement. However, it is still likely that the error was under-estimated. For instance, it was assumed that the calibration between the voltage reading on the oscilloscope and the current in the primary coils was perfect. Clearly, any tiny error in this calibration will play a role in the error of the magnetic field.

For measurements of τ, the largest source of uncertainty came from the voltage measurements. Even with the oscilloscope in `Average` mode, there was a fair amount of fluctuation around an "ideal" exponentially decreasing curve. This error was most pronounced when measuring small peaks for low intensities.

CONCLUSION

Rubidium is a an excellent specimen for studying both the hyperfine structure of atomic states and the process of optical pumping. The Landé g_F factors for ^{85}Rb and ^{87}Rb were found to be 0.335 ± 0.008 and 0.505 ± 0.006, respectively, in good agreement with theoretical predictions of 0.334 and 0.500. At the same time, we were able to measure the Earth's magnetic field in the laboratory to be 0.496 ± 0.029 G. Investigations into characteristic times of establishing steady state polarizations yielded that these times were independent of the light intensity. Finally, we examined the behavior of the spins in the limiting cases of adiabatic and sudden passage through both a resonance and zero field.

There are a couple of ways in which this experiment could be expanded upon. First, data analysis would be faster and more accurate if the oscilloscope could output a data file of the curves instead of requiring reading values from the screen. It would also be interesting to use a stronger magnetic field. This would provide study of the hyperfine spacing between different F levels.

Acknowledgments

I would like to thank Professor Hartill and Johannes Heinonen for their explanations of the basic experimental setup. In addition, I would like to thank Bryan Daniels for his helpful suggestions concerning this report. Special thanks to Tien Le for her continual support.

[1] D. J. Griffiths, *Introduction to Quantum Mechanics* (Prentice Hall, 1995).
[2] K. Gottfried and T. M. Yan, *Quantum Mechanics: Fundamentals* (Springer, 2004), 2nd ed.
[3] R. L. de Zafra, Am. Jour. Phys. **28**, 646 (1960).
[4] R. Benumof, Am. Jour. Phys. **33**, 151 (1965).
[5] R. S. V. D. Jr., P. B. Schwinberg, and H. G. Dehmelt, Phys. Rev. Lett. **59**, 26 (1987).
[6] N. P. Economou, S. J. Lipson, and D. J. Larson, Phys. Rev. Lett. **38**, 1394 (1977).
[7] I. I. Rabi, N. F. Ramsey, and J. Schwinger, Rev. Mod. Phys. **26**, 167 (1954).
[8] R. H. Silsbee (1972).
[9] S. T. Thornton and J. B. Marion, *Classical Dynamics of Particles and Systems* (Thomson Brooks/Cole, 2004), 5th ed.
[10] D. J. Griffiths, *Introduction to Electrodynamics* (Prentice Hall, 1999), 3rd ed.
[11] J. R. Taylor, *An Introduction to Error Analysis* (University Science Books, 1997), 2nd ed.